ANNALS OF GEOPHYSICS, 66, 6, SE644, 2023; doi:10.4401/ag-8934
OPEN ACCESS

Lower Ionospheric variations during the intense tectonic activity in the broader area of Greece on October of 2020

Michael E. Contadakis*[,1], Dimitrios N. Arabelos[1], Christos Pikridas[1], Stylianos Bitharis[1], Emmanuel M. Scordilis[2]

(1) Department of Geodesy and Surveying, Aristotle University of Thessaloniki, Greece
(2) Department of Geophysics, Aristotle University of Thessaloniki, Greece

Article history: received December 28, 2022; accepted February 8, 2023

Abstract

In this paper, we investigate the Lower ionospheric variations from TEC observations during the intense seismic activity of October 2020 in the area of Greece. The data were analysed using both, statistical analysis of TEC variations in order to detect uneven gross variations and Discrete Fourier analysis in order to investigate the TEC turbulence. The results of this investigation indicate that the High-Frequency limit f_o of the ionospheric turbulence content, increases as aproaching the occurrence time of the earthquake, pointing to the earthquake epicenter, in accordance with our previous investigations. We conclude that the Lithosphere Atmosphere Ionosphere Coupling, LAIC, mechanism through acoustic or gravity waves could explain this phenomenology. In addition, the statistical analysis shows an excess greater than 3σ from the mean TEC values, one and seven days before the earthquake. Since no major disturbance of the geomagnetic field occured during these days, we conclude that we probably observed precursory ionospheric variations in accordance to analogous findings from the variation of VH/VHF electromagnetic wave propagrations over strong earthquake areas.

Keywords: Seismicity; Lower Ionosphere; Ionospheric Turbulence; Brownian Walk; Aegean area

1. Introduction

It is argued that tectonic activity during the earthquake preparation period produces anomalies at the ground level which propagate upwards in the troposphere as Acoustic or Standing gravity waves [Miyaki et al., 2002; Hayakawa et al., 2011; Hayakawa, 2011; Hayakawa et al.; 2018].These Acoustic or Gravity waves affect the turbidity of the lower ionosphere, where sporadic Es-layers may appear, and also the turbidity of the F layer. Subsequently the produced disturbance starts to propagate in the ionosphere's waveguide as gravity wave. The inherent frequencies of the acoustic or gravity wave range between 0.003 Hz (period ≈ 5 min) and 0.0002 Hz (period ≈ 100 min), which according to Molchanov et al. [2004, 2006] correspond to the frequencies of the turbulent produced by tectonic activity during the earthquake preparation period. During this propagration the higher frequencies are progressively dumped. Thus observing the frequency content of the ionospheric turbidity we will observe a decrease of the higher limit of the turbitity frequency band.

In this paper we investigate the Lower ionospheric variations from TEC observations during the intense seismic activity of October 2020 in the area of Greece ($35° \leq \varphi \leq 42°$ N, $19° \leq \lambda \leq 29°$ E). The Total Electron Content (TEC) data are been provided by the Hermes GNSS Network managed by GNSS_QC, AUTH Greece, the HxGN/SmartNet-Greece of Metrica S.A, and the EUREF Network. These data were analysed using both, statistical analysis of TEC variations in order to detect uneven gross variations and Discrete Fourier Analysis in order to investigate the TEC turbulence.

2. Seismotectonic Information of the Study Region

Greece and its surroundings are considered among the most seismically active regions of the Alpine-Himalayan Mountain Belt. The high seismic activity of this part of the planet is a result of movements of major and minor lithospheric plates that take place in its vicinity, namely:

a) The western extension of the right-lateral North Anatolian Fault Zone, along which the Anatolian plate rotates to the west [e.g. Oral et al., 1995; Papazacos, 1999],
b) The subduction of the Mediterranean lithospheric plate under Aegean along the Hellenic Arc to the south [e.g. Papazachos and Comninakis, 1970, 1971; McKenzie, 1972, 1978; Dewey and Şengör, 1979; Le Pichon and Angelier, 1979, 1981]
c) The counterclockwise northeastwards move of the Apulian microplate to the west [e.g. Ritsema, 1974; McKenzie, 1972] and
d) The S-SW extension of the Aegean microplate [e.g. Papazachos, 1999]

The tectonic regime of the SE Mediterranean basin is described in Figure 1, where the major and minor lithospheric plates that form it, as well as their movements, are presented.

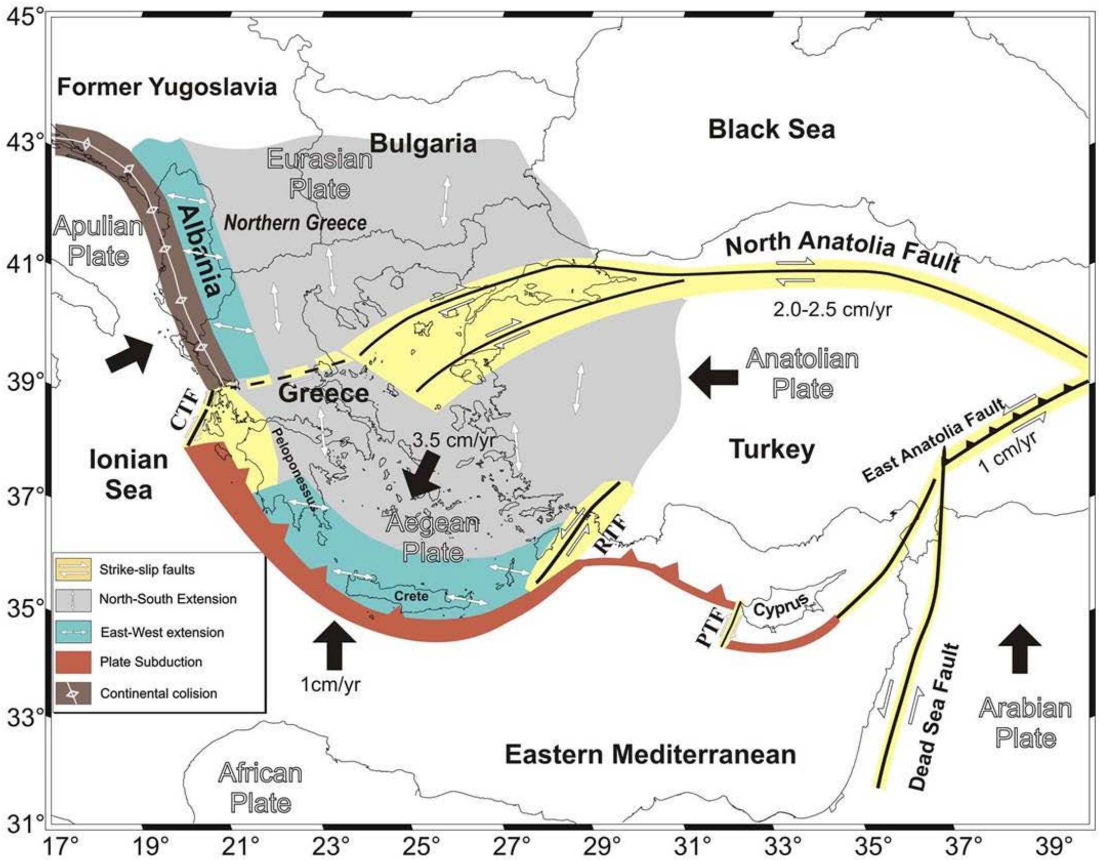

Figure 1. Moves of tectonic plates ruling the active tectonics of Aegean and surroundings [Papazachos et al., 1998].

One strong and five moderate magnitude earthquakes occurred during October of 2020 in eastern Aegean (close to the western coasts of Turkey), in southeastern Aegean and in the Ionian Sea. The first, in chronological order, occurred on October 12 (00:30 GMT) with magnitude Mw = 5.0, to the north of the eastern coasts of Crete Island (west of Karpathos Island) and was followed, a few hours later (04:11 GMT), by another one of relative magnitude (Mw = 5.2) . The third was also of relative magnitude, Mw = 5.2 and occurred on October 21 (23:00 GMT) in the Ionian Sea, south of Zakynthos Island. The fourth and strongest one with magnitude Mw = 7.0 took place on October 30, close to the northern coast of Samos Island ~40 km west of Kusadasi (Turkey). Its strongest aftershocks occurred shortly after, at 11:53 and 15:14 GMT with magnitudes Mw = 5.1 and Mw = 5.0, respectively. Table 1 lists information on the focal parameters of the above six shocks while figure 2 presents a map of the epicenters of the strongest ones, for each of the three seismically excited regions.

	Year	Date	Origin Time (GMT)	Lat (°N)	Lon (°E)	M	Region
1	2020	October 12	00:30:41	35.690	26.314	5.0	Crete-Karpathos
2			04:11:28	35.606	26.276	5.2	
3	2020	October 21	23:00:56	37.230	20.517	5.2	Ionian Sea
4	2020	October 30	11:51:26	37.911	26.815	7.0	Samos Island
5			11:53:54	38.157	26.866	5.1	
6			15:14:57	37.851	26.865	5.0	

Table 1. Focal parameters of the six (five moderate magnitude and the one strong) shallow earthquakes that occurred in the three regions under study. (sources: http://geophysics.geo.auth.gr/ss/bulletins.html, https://www.globalcmt.org)

Figure 2. Map of epicenters of the three strongest earthquakes that occurred in each of the three seismically excited regions of Greece during October 2020.

3. TEC Variation Over mid Latitude of Europe

In this study, the TEC values of several GNSS permanent stations were estimated before and after each of the earthquakes under study. The stations are recording satellite data with a 30-sec observation rate. Most of the stations participate to EPN/EUREF network while some of them belong to local permanent networks of Greece such as HermesNet and HxGN/SmartNet-Greece. Stations with latitudes close to those of the epicenters of these earthquakes were selected.

The TEC values were estimated using the IONosphere Map Exchange (IONEX) Format [Schaer et al., 1998] files where the hourly TEC values from a large network of ten GPS/GNSS stations all over Europe for the test period were estimated.

The processing scenario was applied using the IONEX files that are available at Center for Orbit Determination (CODE), the TEC parameter is modeled with a spherical harmonic expansion up to 15 degree and order 15 referring to a solar-geomagnetic reference frame. The produced ionospheric product is regarded as one of the most precise TEC information.

As it concerns, the TEC estimation for each PRN of the observed satellites included in the selected permanent stations RINEX data, the GPS-TEC software [Seemala and Valladares, 2011] was used considering the receiver and inter-channel biases for different satellites in the receiver. The GPS-TEC software was used to derive TEC values from each dual frequency GPS receiver records. Especially, the GPS-TEC software uses the phase and code values for both L1 and L2 GPS frequencies to eliminate the effect of clock errors and tropospheric water vapor to calculate relative values of slant or line-of-sight TEC. TEC values for each observed satellite such as PRN1 (which is studied in detail) are derived with time resolution of one (1) minute. A single-layer approximation is adopted to convert slant TEC (STEC) into vertical (VTEC) values, where ionospheric piercepoint is considered at an altitude of 350 km above the earth's surface.

For the purposes of our investigation we analyze the variations of TEC over the broader area of Mediterranean before and during the seismic activity of October 2020 in Greece ($19° \leq \lambda \leq 29°$ E, $35° \leq \varphi \leq 42°$ N). To this purpose we use the TEC estimations from the active areas ranging from 0 km to 2678 km, for the time period from 01/10/2020 to 30/10/2020. The selected GPS stations have about the same latitude and are expected to be affected equally from the Equatorial Anomaly as well as from the aurora storms. Table 2 displays the 9 GPS stations, while Figure 3 displays their locations as well as the epicenters of the three strongest events in each activated region. Figure 4 displays the TEC variation over the selected GPS stations during October 2020.

GPS Station	Longitude (°E)	Latitude (°N)	Epicentral dist (km)
SAMOS	26.811	37.924	0.00
ISTA	29.019	41.100	401.532
AUT1	23.004	40.567	440.438
SOFI	23.395	42.556	591.280
ORID	20.794	41.127	626.987
MATG	16.705	40.649	920.457
TLFM	1.223	43.342	2231.920
YEBE	–3.089	40.525	2597.354
MADR	–4.250	40.429	2678.040

Table 2. Distance of GPS stations from the epicenter of the earthquake.

Figure 3. The 9 GPS stations (blue triangles) and the epicenters (red stars) of the 6 earthquakes of Table 1 (the epicenters of the 3 shocks of Samos and of the 2 shocks of Karpathos coincide).

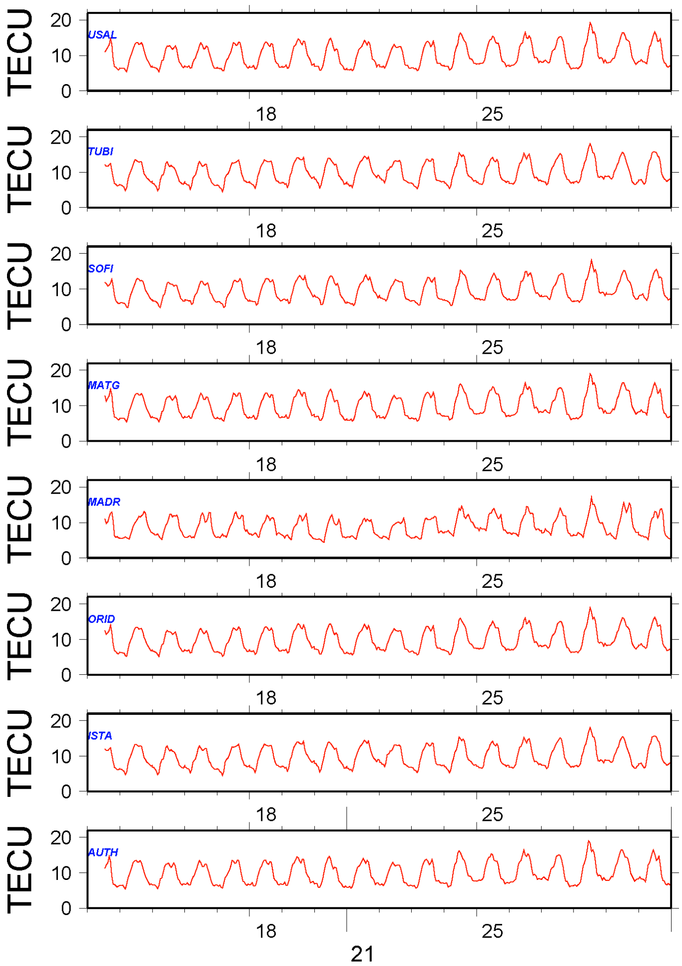

Figure 4. TEC variation over the selected GPS stations during October 2020.

4. Geomagnetic and Solar Activity Indices

The variations of the geomagnetic field were followed by the Dst-index and the planetary kp three-hour indices quoted from the site of the Space Magnetism Faculty of Science, Kyoto University (http://swdcwww.kugi.kyoto-u.ac.jp/index.html) for the time period of our data (Figure 5 presents the Dst-index variations during October 2020).

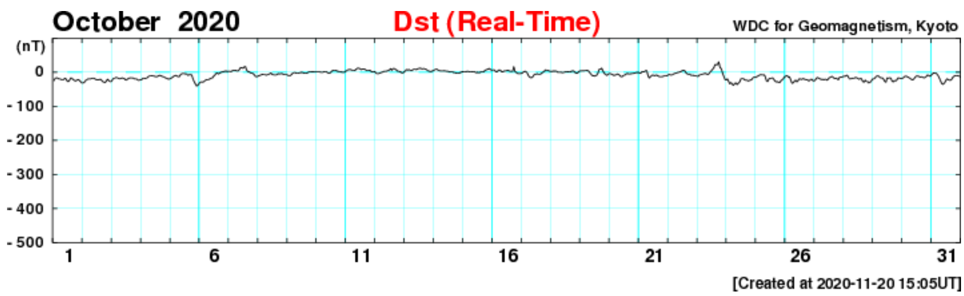

Figure 5. Dst-index variation during October of 2020.

In addition, the Solar activity was very low as it was expected since October 2020 is at the beginning of the solar activity cycle.

5. Data Processing

5.1 Fast Fourier transform analysis

The Power Spectrum of TEC variations will provide information on the frequency content of them. Apart of the well known and well expressed tidal variations, for which the reliability of their identification can be easily inferred by statistical tests, small amplitude space-temporal transient variations cannot have any reliable identification by means of a statistical test. Nevertheless looking at the logarithmic power spectrum, we can recognize from the slope of the diagram whether the contributed variations to the spectrum are random or periodical. If they are random the slope will be 0, which correspond to the white noise, or –2 which correspond to the Brownian walk noise, otherwise the slope will be different, the so called Fractal Brownian walk [Turcotte, 1997]. This means that we can trace the presence of periodical variations in the logarithmic power spectrum of TEC variations. As an example, Figure 6 displays the logarithmic power spectrum of TEC variations over the GPS station of Matera (Italy) on 30/10/2020. It is seen that the slope of the diagram up to the $\log(f_o) = -2$, is $b = 0$ (white noise). For $\log(f_o) = -2$ to $\log(f_o) = -3.3$ is $b = -2$ (Brownian walk noise) and from $\log(f_o) > -3.3$ (fractal Brownian walk noise). This means that for higher than $f_o = \exp(-3.3)$ the TEC variation is random noise. On the contrary, the variation of TEC for lower frequencies contains not random variations, i.e. turbulent. So we conclude that the upper limit of the turbulent band is $f_o = \exp(-3.3) = 0.0247$ cycl/min = > 412.8 μHz. Equivalently, the lower period limit P_o of the contained turbulent is 40.447 minutes. In this analysis we use data from the PRN1 satellite RINEX data and the respective GPS-TEC software (see section 3).

5.2 Simple statistical inspection of TEC variation over Thessaloniki station (AUT1)

In addition to the fractal analysis, a statistical inspection of TEC variation over Thessaloniki on October of 2020 in order to realize if there exists any uneven variation which could be considered as a variation connected to earthquake occurrence. In this analysis we use the data of all the 32 sattelite and the processing scenario was applied using the IONEX files that are available at Center for Orbit Determination, CODE (see Section 3).

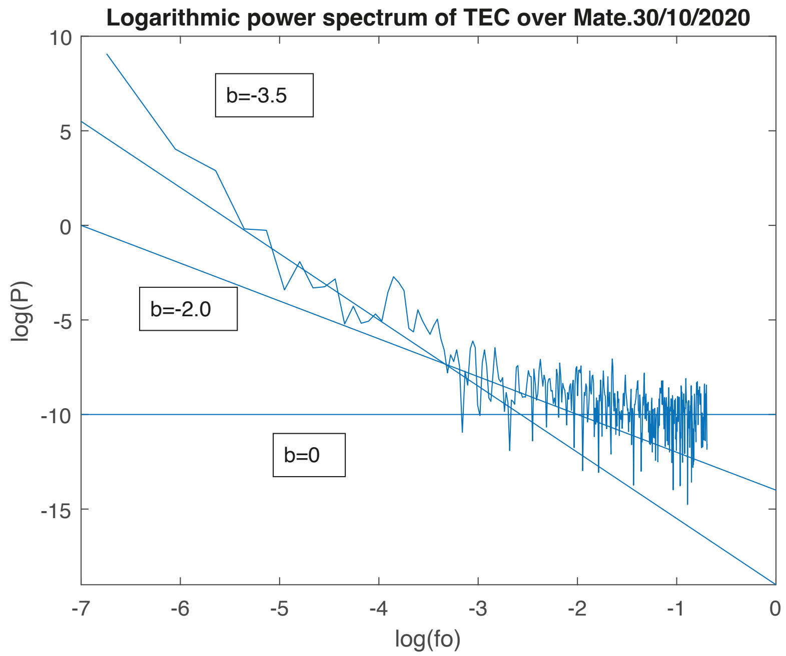

Figure 6. Logarithmic power spectrum of TEC variations over MATE (Matera, Italy) on 30 October 2020.

6. Results

6.1 Fast Fourier transform analysis

Figures 7 and 8 display the variation of the TEC turbulence frequency band upper limit f_o with time and epicentral distance from the Samos main shock of 30/10 2020, while Figures 9 and 10 display the respective variation of the period lower limit P_o. It is shown that a strong dependence of the upper frequency f_o limit (lower period limit P_o) of the ionospheric turbulent band content with time and with epicentral distance is observed. In particular, the closer in time to the origin time of the mainshock,or in space to the active area the higher frequency f_o limit/lower period P_o, is. The observed frequencies (and the respective periods) are in the range of the observed Acoustic Gravity Waves on the occasions of strong earthquakes, which correspond to periods of 30 to 100 min [Molchanov et al., 2004; Molchanov et al., 2005] or 20 to 80 min [Horie et al., 2007].

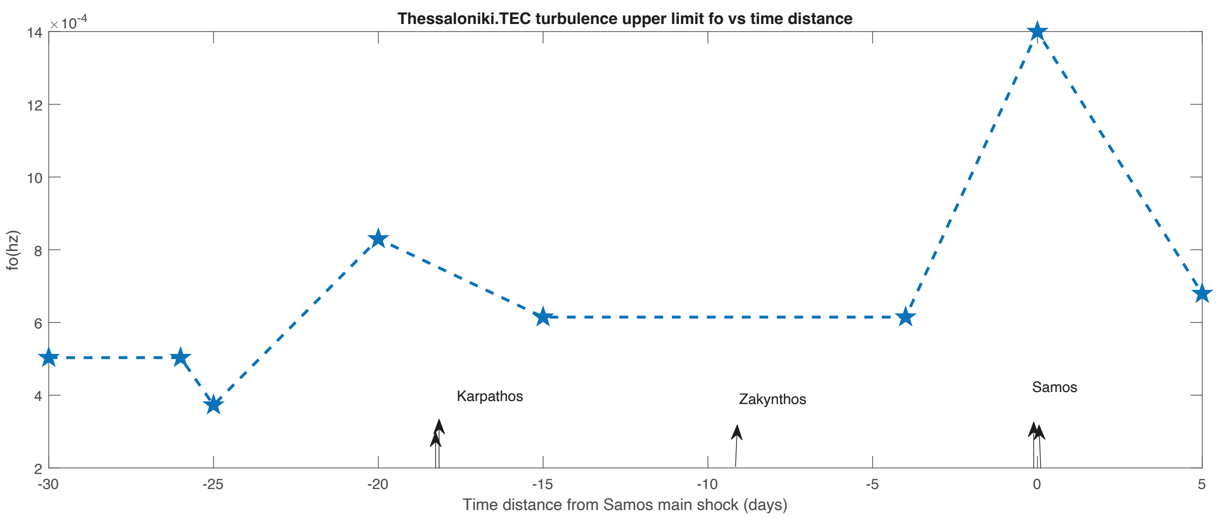

Figure 7. TEC turbulence band upper limit f_o versus time to the Samos main shock.

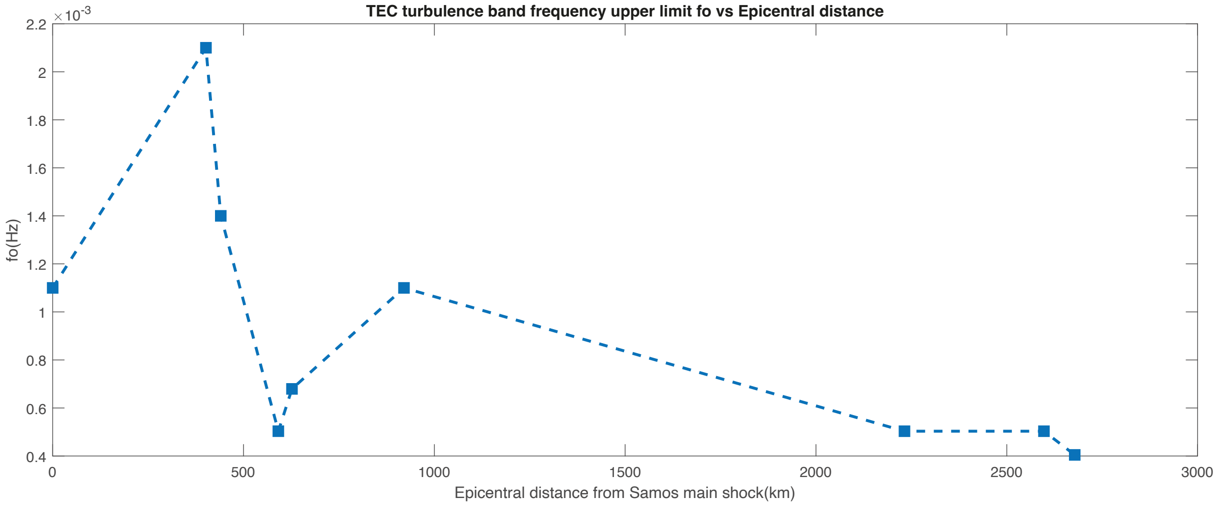

Figure 8. TEC turbulence band upper limit f_o versus epicentral distance from Samos main shock.

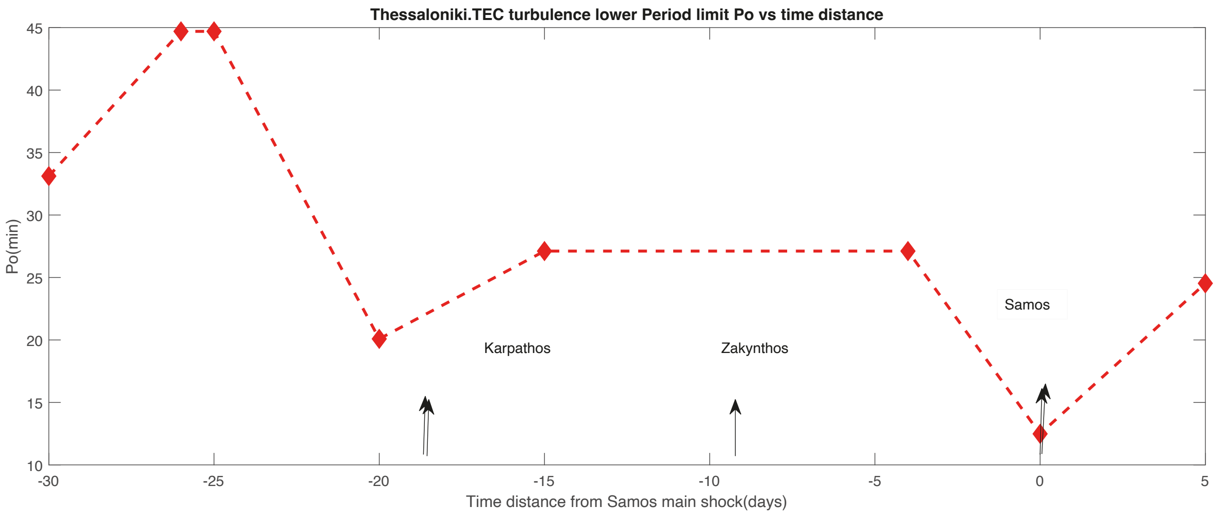

Figure 9. TEC turbulence band lower period limit P_o versus time to the Samos main shock.

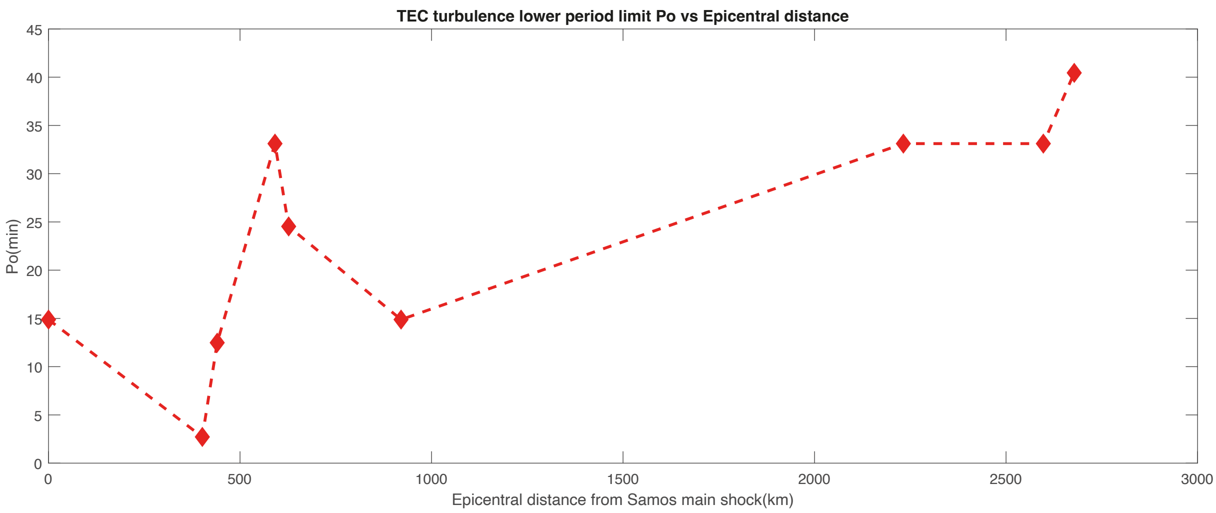

Figure 10. TEC turbulence band lower period limit P_o versus epicentral distance from Samos mainshock.

Hobara et al. [2005] in a study on the ionospheric turbulence in low latitudes concluded that the attribution of the turbulence to earthquake process and not to other sources, i.e. solar activity, storms etc is not conclusive. Nevertheless, in our case, the steady monotonic, time and space, convergence of the frequency band upper limit f_o increment, to the occurrence of the examined strong earthquakes is a strong indication that the observed turbulence is generated by the respective earthquake preparation process.

The qualitative explanation of this phenomenology can be offered on the basis of the Lithosphere Atmosphere Ionosphere Coupling, LAIC: Tectonic activity during the earthquake preparation period produces anomalies at the ground level which propagate upwards in the troposphere as acoustic or standing gravity waves [Hayakawa et al., 2011; Hayakawa, 2011]. These acoustic or gravity waves affect both, the turbulence of the lower ionosphere, where sporadic Es-layers may appear too [Liperovsky et al., 2005], and the turbulence of the F-layer. Subsequently, the produced disturbance starts to propagate in the ionosphere's waveguide as gravity wave and the inherent frequencies of the acoustic or gravity waves can be traced on TEC variations [i.e. the frequencies between 0.003 Hz (period 5 min) and 0.0002 Hz (period 100 min)], which, according to Molchanov et al. [2004, 2005] and Horie et al. [2007], correspond to the frequencies of the turbulent induced by the LAIC coupling process to the ionosphere. As we move far from the disturbed point, in time or in space, the higher frequencies (shorter wavelength) variations are progressively attenuated.

6.2 Simple statistical inspection of TEC variation over Thessaloniki station (AUT1)

In addition to the Discrete Fourier analysis of the ionospheric turbulence band, a simple statistical inspection of TEC variation on October 2020, over Thessaloniki station, one of the nearest EPN/EUREF stations to the Samos earthquake epicenter, was performed.

Figure 11 displays TEC variation over Thessaloniki in October 2020 while Figure 12 displays the daily Mean Max and Minumum TEC values during the same time period. The monthly tidal variation is apparent from the TEC variation as well as from the Maximum and Mean daily variation. The same fact is shown in Figure 13 where the TEC variation is compared with the mean TEC variation in October 2020. Nevertheless, extremely high TEC values after 15 of October are observed. Thus we check if these values exceed the mean+2σ value. This is shown in Figures 14 and 15. From these figures we realize that on 21/10 and 29/10 TEC values exceed this limit. Since the Geomagnetic field is very quiet (see Figure 5), the solar activity is minimum and the Auroral Electrojets are absend in 21/10 and weak in 29/10, we conclude that the high TEC values include, most probably, an earthquake related contribution.

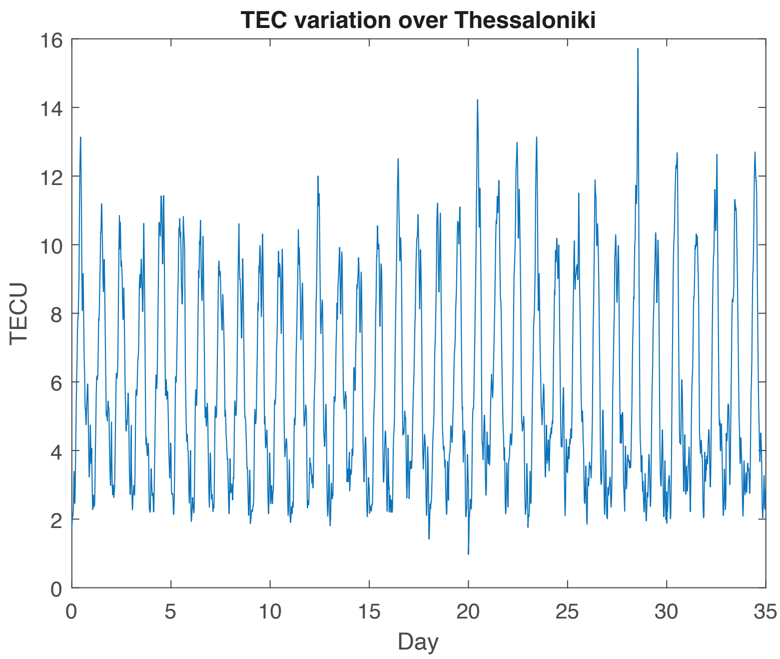

Figure 11. TEC variations over Thessaloniki GPS station (AUT1) in October of 2020.

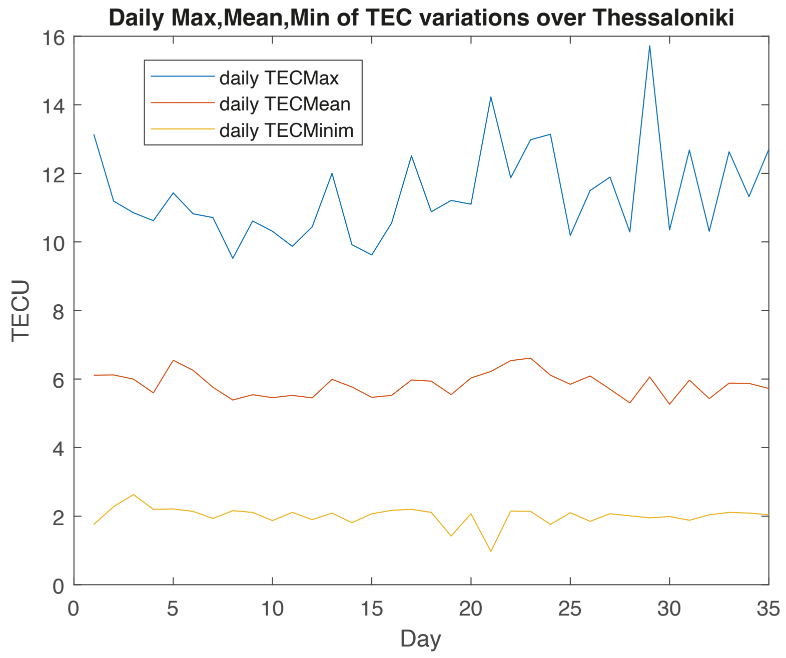

Figure 12. Thessaloniki GPS : Daily max, min and mean TEC values during October of 2020.

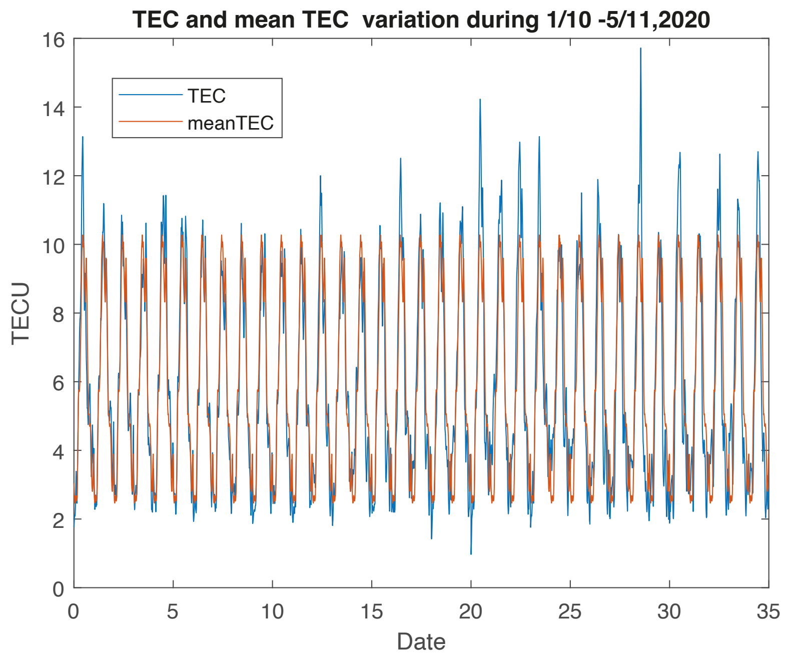

Figure 13. Thessaloniki GPS : TEC and TEC Mean variation during October of 2020.

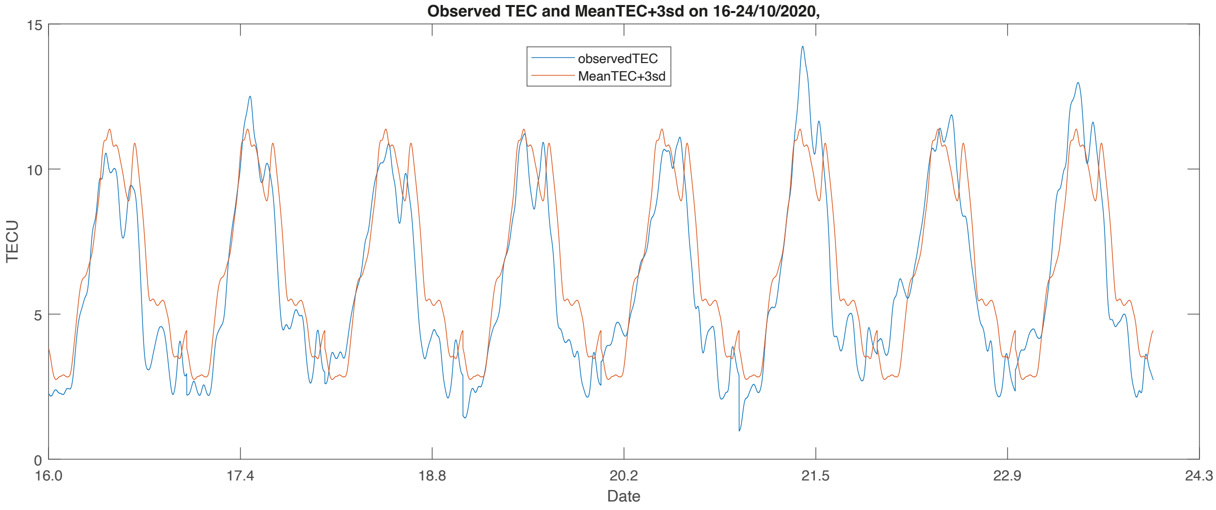

Figure 14. Thessaloniki GPS : TEC and TEC mean+3σ variation during 16-24 of October 2020.

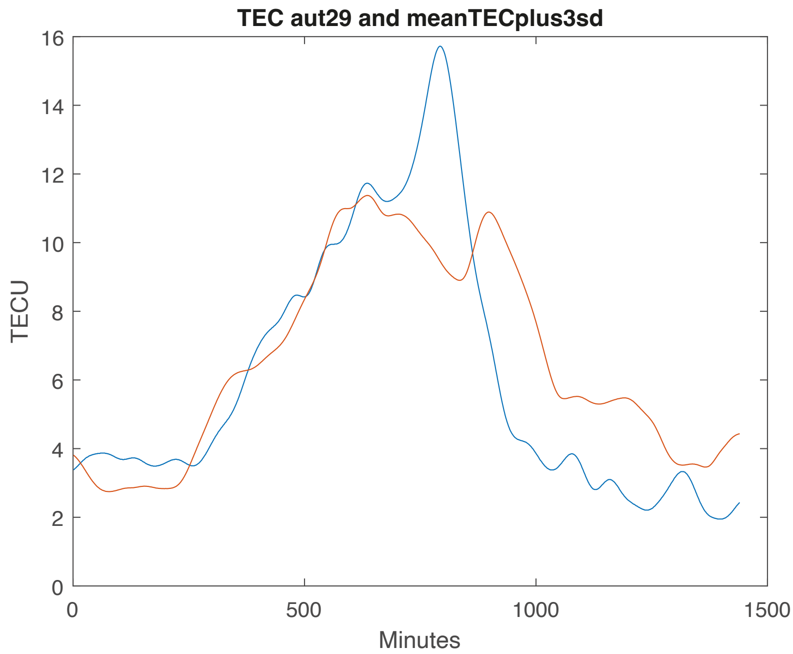

Figure 15. Thessaloniki GPS : TEC and TEC mean+3σ variation during 29 of October, 2020.

7. Conclusions

The results of this investigation indicate that the High-Frequency limit f_0 of the ionospheric turbulence content, increases as aproaching the occurrence time of the earthquake, pointing to the earthquake epicenter, in accordane to our previous investigations [Contadakis et al., 2015; Scordilis et al., 2020]. We conclude that the LAIC mechanism through acoustic or gravity waves could explain this phenomenology. Furthermore, the statistical analysis shows an excess of more than 3σ in the mean TEC values, one and seven days before the earthquake. Since no significant perturbation of the geomagnetic field occured during these days, we conclude that we probably observed precursory ionospheric variations similar to analogous findings from the variation of VH/VHF electromagnetic wave propagration over strong earthquake regions [e.g. Biagi et al., 2019]. Furthermore, a simple statistical investigation of the October 2020 TEC variation over the Thessaloniki station (AUT1), one of the closest EPN/EUREF stations to the epicenter of the Samos earthquake, shows that the TEC variation during the last 15 days before the earthquake is associated probably with this strong event.

References

Biagi, P.F., R. Colella, L. Schiavulli, A. Ermini, M. Boudjada, H. Eichelberger, K. Schwingenschuh, K. Katzis, M.E. Contadakis, C. Skeberis, I.A. Moldovan and M. Bezzeghoud (2019). The INFREP Network: Present Situation and Recent Results. Open J. Earthq. Res., 8, 101-115.

Bruyninx, C., J. Legrand, A. Fabian and E. Pottiaux (2019). GNSS metadata and data validation in the EUREF Permanent Network, GPS Solut. 23, 106, https://doi.org/10.1007/s10291-019-0880-9.

Contadakis, M.E., D.N. Arabelos, G. Vergos, S.D. Spatalas and E.M. Scordilis (2015). TEC variations over the Mediterranean before and during the strong earthquake (M = 6.5) of 12th October 2013 in Crete, Greece, Physics and Chemistry of the Earth, Volume 85, 9-16.

Dewey, J.F. and A.M.C. Sengör (1979). Aegean and surrounding regions: complex multiplate and continuum tectonics in a convergent zone, Geol. Soc. Am. Bull., 90, 84-92.

Hayakawa, M. (2011). On the fluctuation spectra of seismo-electromagnetic phenomena, Nat. Hazards Earth Syst. Sci., 11, 301-308.

Hayakawa, M., Y. Kasahara, T. Nakamura, Y. Hobara, A. Rozhnoi, M. Solovieva, O.A. Molchanov and V. Korepanov (2011). Atmospheric gravity waves as a possible candidate for seismo-ionospheric perturbations, J. Atmos.Electr., 32, 3, 129-140.

Hayakawa, M., T. Asano, A. Rozhnoi and M. Solovieva (2018). Very-low- and low-frequency sounding of ionospheric perturbations and possible association withearthquakes, in “Pre-earthquake Processes: A multidisciplinary approach to earthquake prediction studies”, Ed. by D. Ouzounov et al., 277-304, AGU Book, Wiley.

Hobara, Y., F. Lefeuvre, M. Parrot and O.A. Molchanov (2005). Low-latitude ionospheric turbulence observed by Aureol-3 satellite, Annales Geophysicae, 23, 1259-1270.

Horie, T., S. Maekawa, T. Yamauchix, M. Hayakawa (2007). A possible effect of ionospheric perturbations associated with the Sumatra earthquake, as revealed from subionospheric very-low-frequency (VLF) propagation (NWC-Japan), International Journal of Remote Sensing, vol. 28, issue 13, 3133-3139.

Kruse, S. and L.H. Royden (1994). Bending and unbending of an elastic lithosphere: the Cenozoic history of the Apennine and Dinarideforedeep basins. Tectonics, 13, 278-302.

Le Pichon, X. and J. Angelier (1979). The Hellenic arc and trench system: a key to the neotectonic evolution of the eastern Mediterranean area, Tectonophysics, 60, 1-42.

Le Pichon X. and J. Angelier (1981). The Aegean Sea, Philos. Trans. Royal Soc. London, A300, 357-372.

McKenzie, D.P. (1972). Active tectonics of the Mediterranean region. Geophys, J. R. Astr. Soc., 30, 109-185.

McKenzie, D.P. (1978). Active tectonics of the Alpine-Himalayan belt: the Aegean Sea and surrounding regions, Geophys. J. R. Astr. Soc., 55, 217-254.

Miyaki, K., M. Hayakawa and O.A. Molchanov (2002). The role of gravity waves in the lithosphere-atmosphere-ionosphere coupling, as revealed from the subionospheric LF propagation, in “Seismo Electromagnetics: Lithosphere-Atmosphere-Ionosphere Coupling”, Ed. by M. Hayakawa and O.A. Molchanov, TERRAPUB, Tokyo, 229-232.

Molchanov, O., P.F. Biagi, M. Hayakawa, A. Lutikov, S. Yunga, D. Iudin, S. Andreevsky, A. Rozhnoi, V. Surkov, V. Chebrov, E. Gordeev, A. Schekotov and E. Fedorov (2004). Lithosphere-atmosphere-ionosphere coupling as governing mechanism for preseismic short-term events in atmosphere and ionosphere, Nat. Hazards Earth Syst. Sci., 4, 5/6, 757-767.

Molchanov, O., A. Schekotov, M. Solovieva, E. Fedorov, V. Gladyshev, E. Gordeev, V. Chebrov, D. Saltykov, V.I. Sinitsin, K. Hattori and M. Hayakawa (2005). Near seismic effects in ULF fields and seismo-acoustic emission: statistics and explanation, Nat. Hazards Earth Syst. Sci., 5, 1-10.

Oral, M.B., R.E. Reilinger, M.N. Toksoz, R.W. King, A.A. Barka, J. Kiniki and D. Lenk (1995). Global Positioning System offers evidence of plate motions in Eastern Mediterranean, EOS, 76, 9-11.

Papazachos, B.C. and P.E. Comninakis (1970). Geophysical features of the Greek Island Arc and Eastern Mediterranean Ridge. Com. Ren. Des Seances de la Conference Reunie a Madrid, 1969, 16, 74-75.

Papazachos, B.C. and P.E. Comninakis (1971). Geophysical and tectonic features of the Aegean arc. J. Geophys. Res., 76, 8517-8533.

Papazachos, B.C., E.E. Papadimitriou, A.A. Kiratzi, C.B. Papazachos and E.K. Louvari (1998). Fault plane solutions in the Aegean and the surrounding area and their tectonic implications, Boll. Geof. Teor. Appl., 39, 199-218.

Papazachos, C.B. (1999). Seismological and GPS evidence for the Aegean-Anatolia interaction. Geophys. Int. Lett., 26, 2653-2656.

Ritsema, A.R. (1974). The earthquake mechanism in Balkan region. Inst. Sci. Rep., 74, 1-36.

Schaer, S., W. Gurtner and J. Feltens (1998). "IONEX: The ionosphere map exchange format version 1."Proceedings of the IGS AC workshop", Darmstadt, Germany. Vol. 9. No. 11.

Scordilis, E.M., M.E Contadakis, F. Vallianatos and S. Spatalas (2020). Lower Ionospheric turbulence variations during the intense tectonic activity in Eastern Aegean area, Annals of Geophysics, 63, 5, PA544.

Seemala, G.K. and C.E. Valladares (2011), Statistics of total electron content depletions observed over the South American continent for the year 2008, Radio Science, 46, RS5019, doi:10.1029/2011RS004722.

Turcotte, D.L. (1997). Fractal and Chaos in Geology and Geophysics (2nd Edition), Cambridge University Press, Cambridge U.K.

***CORRESPONDING AUTHOR: Michael E. CONTADAKIS**,
Department of Geodesy and Surveying, Aristotle University of Thessaloniki, Greece
e-mail: mcont@topo.auth.gr